JOURNAL OF MATERIALS SCIENCE 20 (1985) 3167 - 3176

Electrical transport in light rare-earth vanadates

KANCHAN GAUR, H. B. LAL
Department of Physics, University of Gorakhpur, Gorakhpur-273001, India

This paper reports electrical transport studies of rare-earth vanadates (RVO_4 with R = Ce, Pr, Nd, Sm, Eu and Gd), prepared by solid state reaction and characterized by X-ray diffraction studies. TGA study (300 to 1200 K) shows no weight loss; possible phase transitions in the range 1075 to 1300 K have been indicated by DTA studies. All these vanadates are typical semiconducting compounds with room temperature electrical conductivity (σ) lying between 10^{-4} and $10^{-2}\Omega^{-1}m^{-1}$. Measurements of σ and the Seebeck coefficient (S) are reported in the temperature interval 400 to 1200 K. Two linear regions 400 to T_1 K and T_1 to T_2 K have been obtained from the log σ against T^{-1} as well as the S against T^{-1} plots followed by a peak around T_3 and minima around T_4 K. $T_4 > T_3 > T_2 > T_1$ are different for different vanadates. It has been concluded that in the interval 400 to T_1 K, conduction is of the extrinsic hopping type with Ce^{4+} in $CeVO_4$, Pr^{4+} in $PrVO_4$ and V^{4+} in Nd to Gd vanadates as dominant defect centres. In the temperature interval T_1 to T_2 K, the conduction has been shown to be of the intrinsic band type in all vanadates with polarons of intermediate coupling strength as the dominant charge carriers. Above T_2 all vanadates tend to become metallic, but before this is achieved the phase change makes the conductivity smaller. T_4 is close enough to the temperature corresponding to the DTA peak to be termed the phase transition temperature.

1. Introduction

Mixed oxides of rare-earth and iron group elements are well known for their wide ranging physical properties. Among these vanadates of rare-earth (RVO_4, R standing for La–Lu) form a group of compounds revealing interesting structural and magnetic transformations [1]. Recently we have reported unusual magnetic behaviour of gadolinium [2], light [3] and heavy [4] rare-earth vanadates at higher temperatures and electrical transport and semiconductor-semimetal transition in $LaVO_4$ [5]. This interesting and, to some extent, unusual behaviour of these compounds prompted us to investigate the electrical transport properties of the whole series of rare-earth vanadates. As a part of the plan this paper reports the electrical transport properties of light rare-earth (R = Ce, Pr, Nd, Sm, Eu and Gd) vanadates. All these vanadates have a tetragonal unit cell with cell parameters as given in Table I at room temperature [6].

2. Material preparation and experimental techniques

The details for the preparation of all rare-earth vanadates, including starting materials, have already been reported in our earlier publications

TABLE I Unit cell parameters of RVO_4 at 298 K (unit cell tetragonal)

R	Unit cell parameters	
	a_0(nm)	c_0(nm)
Ce	0.7399	0.6496
Pr	0.7367	0.6468
Nd	0.7329	0.6436
Sm	0.7266	0.6394
Eu	0.7237	0.6368
Gd	0.7211	0.6350

0022–2461/85 $03.00 + .12

[2–4]. The X-ray diffraction patterns were recorded using powdered samples employing Cu$K\alpha$ (λ = 0.154 050 nm) radiation and evaluated unit cell parameters were almost the same as those given in Table I. DTA and TGA studies were performed at a heating rate of 10° C min^{-1}. The electrical conductivity (σ) and the Seebeck coefficient (S) measurements were carried out using sample holders and procedures as described in several publications of our group [7–9].

3. Results

Measurements of σ and S were performed on pressed pellets because of the difficulty of growing large single crystals of these compounds needed for such measurements due to their high melting point and our limited facilities. In pellets, grain boundaries and air pores considerably reduce conductivity and often measurements on them do not reflect the bulk value for the material. It is not possible to eliminate them completely; however, pellets can be prepared in such a way that these effects are considerably reduced and in such a situation the bulk value for the material can be obtained by employing a suitable correction. The first requirement in this direction is to make pellets of uniform density. This has been achieved by using a proper steel die and keeping t^2/A (where t is the thickness and A the face area of the pellet) ratio less than 4, as fixed by other workers [7–10]. Air pores are considerably reduced if these uniform pellets are made using fine grain powders at higher pelletizing pressure (P) and sintered at higher temperature for longer times. Normally, pellets made at $P > 6 \times 10^8 N m^{-2}$ have a density close enough (85% to 90%) to the X-ray density of the material. The grain boundary effect on pellets made at such high pressures is considerably reduced. This fact is evident from the independence of a.c. electrical conductivity from signal frequency (50 to 10^4 Hz). Electrodes on pellet faces also play a significant role in σ and S measurements. For both measurements the stringent criterion is to have ohmic contact between electrode and pellet interfaces. To investigate the nature of the contact, the d.c. current density (J) through the pellets was recorded as a function of applied electric field (E) for platinum electrode. The plots (not shown) are almost linear right from $E = 0$ in a few cases and above a certain value of E in others. Thus contact between pellet and electrode interfaces, except at very low fields, is ohmic. In the measurement of σ at different temperatures, we used well sintered pellets made at higher pelletizing pressures ($P > 6 \times 10^8 N m^{-2}$) keeping E in the range where contact between pellet–electrode faces was ohmic.

Both the Seebeck coefficient and electrical conductivity of a few pellets of each compound were measured at different temperatures. σ measurement shows a typical hysteresis around certain temperatures marked as T_3 and T_4. In the cooling cycle, the peak normally observed at T_3 is reduced. However, at other temperatures, σ values are almost the same in heating and cooling cycles. The Seebeck coefficient for each RVO_4 is essentially independent of thermal history and the shelf life of the pellet, and is reproducible to within $\pm 5\%$.

Figs. 1 to 3 show the plots of log σ and S against T^{-1} for cerium and praseodymium, neodymium and samarium, and europium and gadolinium vanadates, respectively. The log σ against T^{-1} plots are almost linear from 400 K to a certain temperature, T_1. Similar linear plots are obtained between S and T^{-1} in the temperature range 400 to T_1'K. The variation of σ and S with T^{-1} below T_1 (T_1' for S) can be represented by general relations

$$\sigma = \sigma_0 \exp(-E_a/kT) \quad (1)$$

and

$$S = \frac{\eta}{eT} + H \quad (2)$$

where σ_0 and H are constants, E_a is the activation energy, k is Boltzmann constant, e is electronic charge and η is the slope of S–T^{-1} line.

The variations of log σ and S with T^{-1} in the temperature range $T_1 < T < T_2$ ($T_1' < T < T_2'$ for S) can also be represented by Equations 1 and 2 with different values of σ_0, E_a, and H. The summarized results of σ and S together with respective constants are given in Tables II and III, respectively. Within the temperature range 400 to T_1 K, σ values decrease as we go down in series from cerium to neodymium. It has a minimum value for neodymium and then increases slowly as we proceed further in the series from samarium to gadolinium. No time dependence was observed in J values at a fixed temperature.

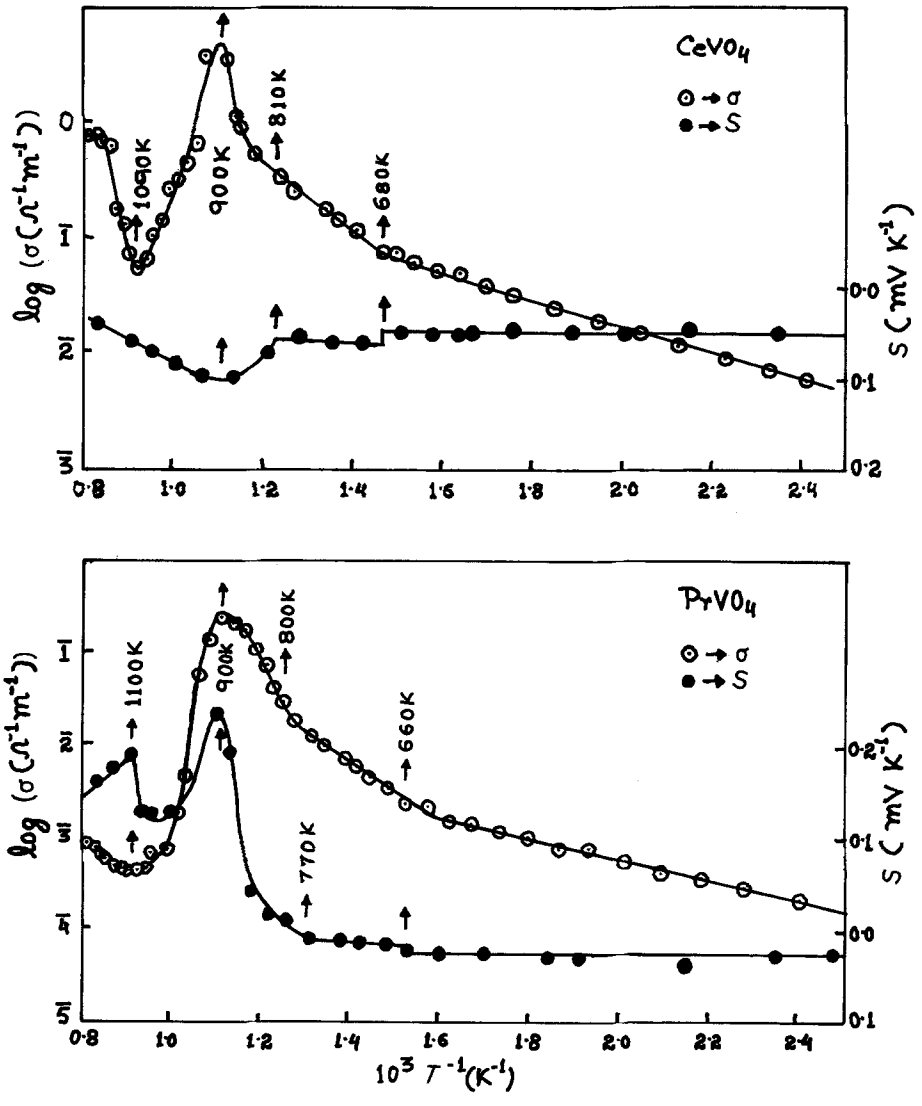

Figure 1 Variation of log σ and S with inverse of absolute temperature ($T^{-1}K^{-1}$) for cerium and praseodymium vanadates.

This indicates that charge carriers in these solids are electronic (i.e. either electrons or holes). Above T_2, the variations of log σ and S with T^{-1} do not remain linear. They yield a peak around a temperature T_3 (T_3' for S). On the higher side of T_3, σ values decrease with increase in temperature, yield a minimum value at $T_4 (T_4 > T_3)$ and beyond T_4 it again increases with temperature. The break temperatures T_1 and T_2 are not exactly the same as those obtained from log σ and S against T^{-1} plots. The difference is due to different conditions in the measurements of σ and S. In the former, the sample was kept in a uniform thermal state, whereas in the latter it was subjected to a thermal gradient.

S values are negative for $CeVO_4$ in the whole temperature range and for $PrVO_4$ in the temperature range 400 to 785 K but above this temperature it becomes positive. For neodymium, samarium europium and gadolinium vanadates the sign of the Seebeck coefficient is positive in the entire temperature range. Thus as per our sign convention [11] in which the sign of the charge carrier is taken as being opposite to the sign of S, the electrons are the dominant charge carriers in neodymium, samarium, europium and gadolinium vanadates over the entire studied temperature range (400 to 1250 K). In $PrVO_4$, they are holes up to 785 K and electrons above this temperature. In $CeVO_4$, charge carriers are holes over the entire temperature range.

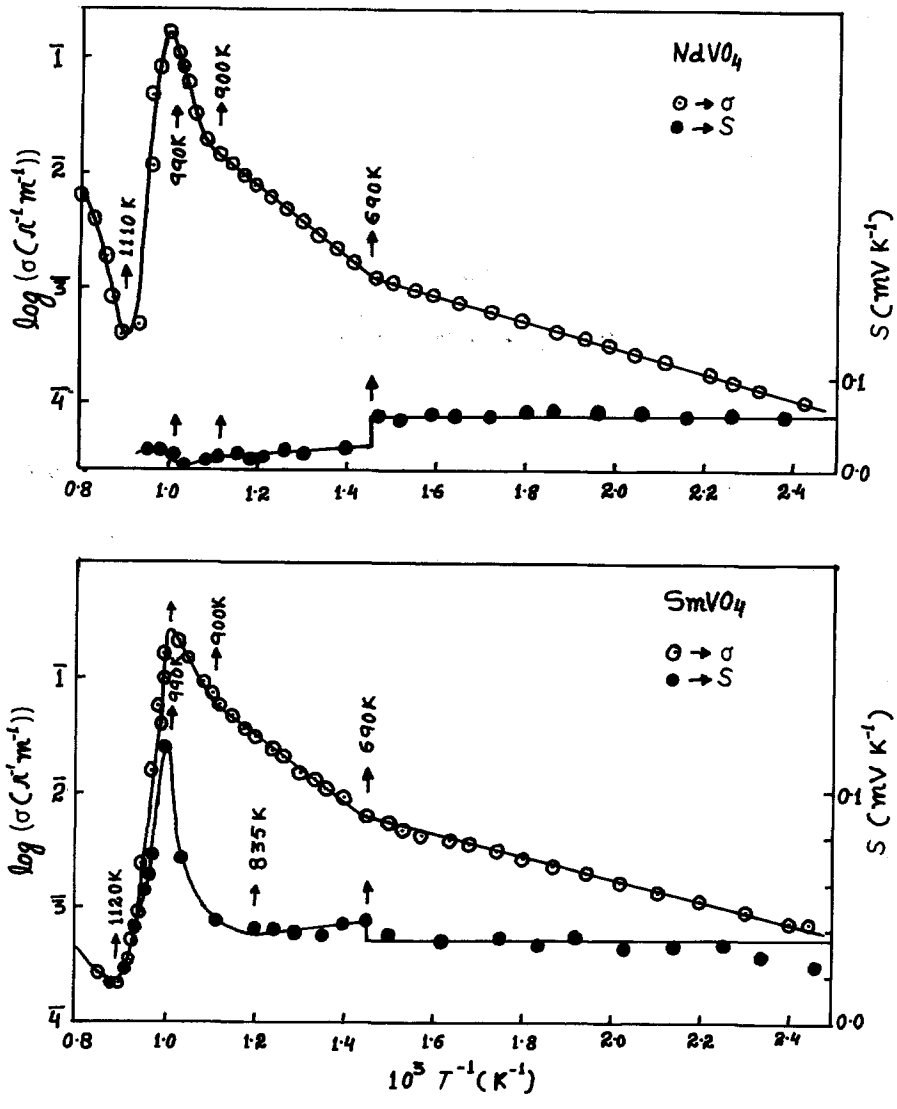

Figure 2 Variation of log σ and S with inverse of absolute temperature for neodymium and samarium vanadates.

TABLE II Summarized results of electrical conductivity (σ) measurements for RVO_4

R	σ, at 500 K ($\Omega^{-1}m^{-1}$)	Linear range $T < T_1$		T_1 (K)	Linear range $T_1 < T < T_2$		T_2 (K)	T_3 (K)	T_4 (K)
		σ_0 ($\Omega^{-1}m^{-1}$)	E_a (eV)		σ_0 ($\Omega^{-1}m^{-1}$)	E_a (eV)			
Ce	1.91×10^{-2}	2.331	0.21	680	1.94×10^{3}	0.62	810	900	1090
Pr	5.89×10^{-4}	0.096	0.22	660	2.15×10^{2}	0.64	800	900	1100
Nd	3.02×10^{-4}	0.049	0.22	690	4.16×10^{1}	0.65	900	990	1110
Sm	1.70×10^{-3}	0.984	0.20	690	1.37×10^{2}	0.66	900	990	1120
Eu	5.75×10^{-3}	0.953	0.22	715* (740)	4.10×10^{2}	0.67	910	1000	1125
Gd	7.94×10^{-3}	1.097	0.22	555* (745)	1.42×10^{2}	0.68	920	1000	1130

*log σ against T^{-1} curve becomes flat above this temperature and remains so until the temperatures given in parentheses.

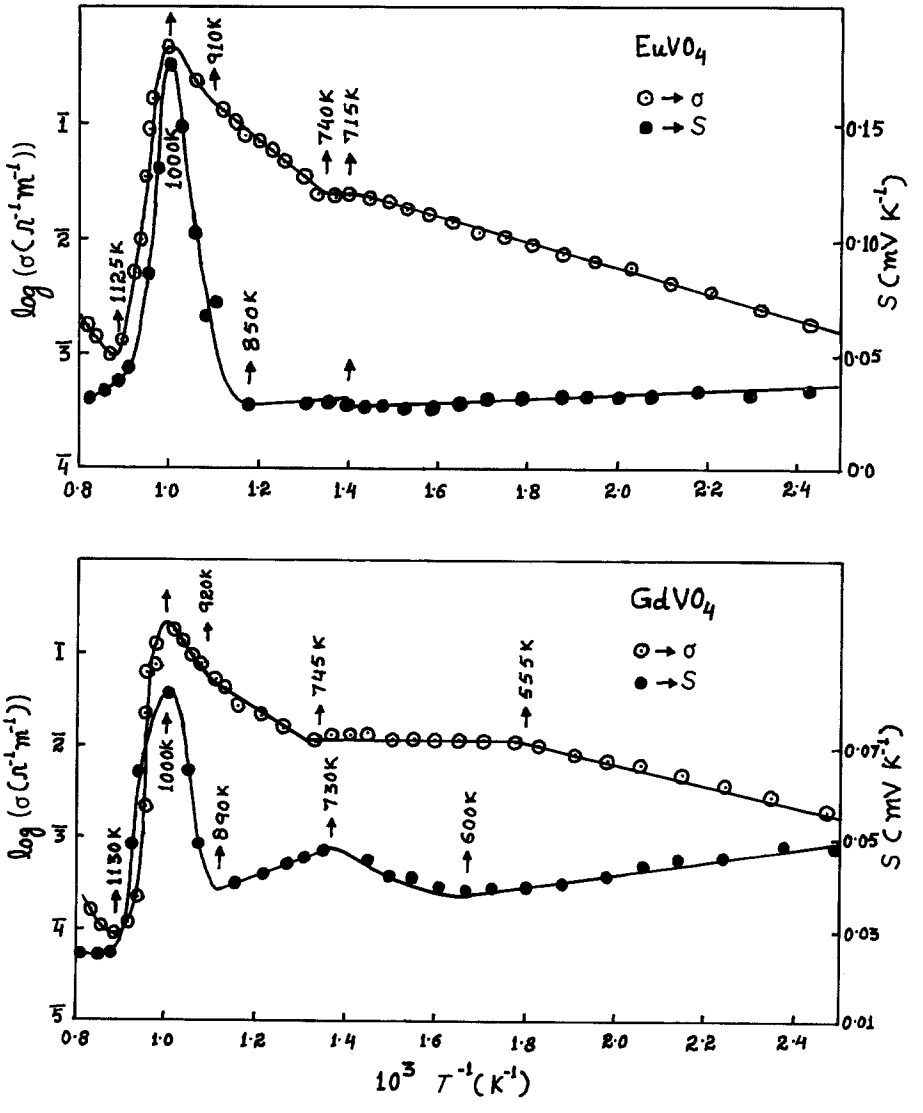

Figure 3 Variation of log σ and S with inverse of absolute temperature for europium and gadolinium vanadates.

TABLE III Summarized result of Seebeck coefficient measurement for RVO_4

R	S at 500 K (mV K^{-1})	Linear range $T < T_1'$		T_1' (K)	Linear range $T_1' < T < T_2'$		T_2' (K)	T_3' (K)	T_4' (K)
		η (mV)	H (mV K^{-1})		η (mV)	H (mV K^{-1})			
Ce	−0.050	0	−0.050	680	−0.025	−0.048	810	900	–
Pr	−0.025	0	−0.025	660	−0.025	+0.003	770	900	1100
Nd	+0.060	0	+0.060	690	+0.025	+0.007	900	990	–
Sm	+0.036	0	+0.036	690	+0.025	+0.025	835	990	1120
Eu	+0.032	+0.008	+0.030	715	+0.002	+0.028	850	1000	–
Gd	+0.043	+0.013	+0.038	600	+0.035	+0.021	890	1000	1130

4. Discussion

The log σ against T^{-1} plots (Figs. 1 to 3) for all vanadates yield two linear regions in the temperature range 400 to T_1 K and T_1 to T_2 K with a slope of ~ 0.22 and ~ 0.62 eV, respectively. In the first region, S remains practically constant indicating that charge carriers for conduction are not thermally generated but are constant. This may happen when charge carriers are localized on defect centres and conduct via a hopping mechanism. It is worth mentioning in this respect that our magnetic study [3] has indicated the presence of V^{4+} defect centres in RVO_4. We propose, as we had already done for $LaVO_4$ [5], that hopping of electrons from V^{4+} defect centres to V^{5+} normal sites is the prominent conduction mechanism in neodynium, samarium, europium and gadolinium vanadates in the temperature range 400 to T_1 K. However, in $CeVO_4$ and $PrVO_4$ the dominant charge carriers in this temperature range are holes against the electrons expected from V^{4+} centres. This means that there exists a very small number of V^{4+} centres in Ce and Pr vanadates. This may be true, as V^{4+} centres are formed due to oxygen deficiency in RVO_4, whose chances are very small in $CeVO_4$ and $PrVO_4$. These vanadates are prepared using the solid state reactions

$$4CeO_2 + 2V_2O_5 \rightarrow 4CeVO_4 + O_2 \quad (3)$$

$$Pr_6O_{11} + 3V_2O_5 \rightarrow 6PrVO_4 + O_2 \quad (4)$$

In the light of the above equations, oxygen deficiency and thus the existence of V^{4+} centres is not expected in cerium and praseodymium vanadates. However, both cerium and praseodymium have a tendency to be present in their respective compounds as tetravalent (Ce^{4+} and Pr^{4+}) ions. Thus, the existence of Ce^{4+} centres in $CeVO_4$ and Pr^{4+} centres in $PrVO_4$ is quite possible. They can take part in conduction, as a hole from a Ce^{4+} (or Pr^{4+}) centre can hop to a Ce^{3+} (or Pr^{3+}) normal site. As holes are the dominant charge carriers in Ce and Pr vanadates, the mechanism described above may be the dominant conduction mechanism in these solids. At higher temperatures (T_1 to T_2) the σ for RVO_4 is expected to be intrinsic. Furthermore, all rare-earth vanadates are semiconducting solids, hence it seems appropriate to explain electrical conduction in these solids using a common broad energy band model. The relevant bands which may be important are empty R^{3+}: 5d, V^{5+}: 4s and V^{5+}: 3d bands, partially filled R^{3+}: $4f^n$ levels (or extremely narrow bands) and completely filled O^{2-}: 2p band. The magnitude of electrical conductivity in the RVO_4 studied is of the order of V_2O_5 [12] and is several orders of magnitude larger than in corresponding R_2O_3 [13]. Thus R^{3+}: 5d band should not come in the picture in the electrical conduction of these solids. The semi-empirical model proposed by Goodenough [14] is helpful in deciding relative positions of these bands. Relevant optical data are, however, not available on these materials to apply it in correct perspective. In any case the V^{5+}: 4s band should be separated with the V^{5+}: 3d band and should lie few electron volt above it. RVO_4 are very stable and therefore the O^{2-}: 2p band should lie below the V^{5+}: 3d band. The position of filled R^{3+}: $4f^n$ levels is not very certain but they must lie close to the top of the O^{2-}: 2p band. They will, however, shift sequentially down until they are half filled. A general schematic energy band diagram of RVO_4 is shown in Fig. 4. Based on this energy band picture, the intrinsic conduction in RVO_4 will occur by the following processes:

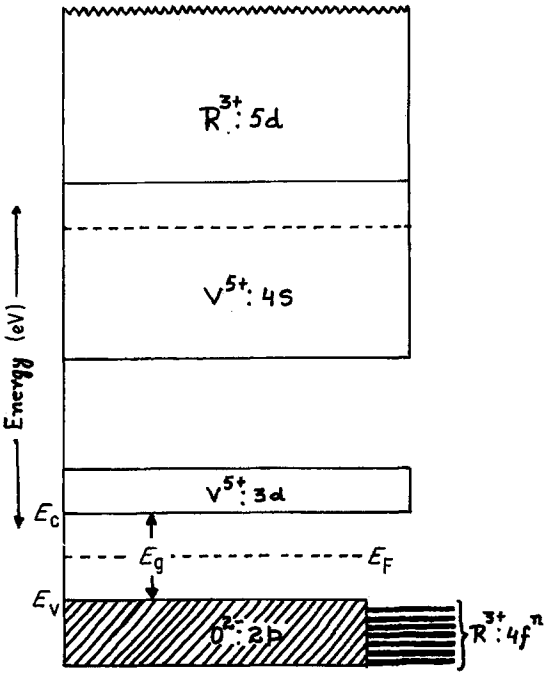

Figure 4 Schematic band diagram for RVO_4.

1. Electrons from the filled O^{2-}: 2p band are excited to the empty V^{5+}: 3d band leaving holes in the former. The thermally generated electrons in the V^{5+}: 3d (conduction) band and holes in the O^{2-}: 2p (valence) band will conduct in their respective bands. Both V^{5+}: 3d and O^{2-}: 2p bands will be narrow and may be split by a crystal field making them still narrower. This will make the mobility of charge carriers in both bands smaller.

2. In case of $4f^n$ levels lying between oxygen 2p and vanadium 3d bands, electrons may also be excited from the $4f^n$ level to the V^{5+}: 3d band. In this case the dominant charge carriers will be electrons in the vanadium 3d band, as the holes created in $4f^n$ levels will be almost localized. The plot of log σ against T^{-1} will also be linear with a slope corresponding to an energy of $W/2$, where W is the difference of energy between the $4f^n$ level and the bottom of the V^{5+}: 3d band. However, if this is true, the linear variation of S with T^{-1} should also yield a slope corresponding to energy $W/2$. This is not true, as the experimentally observed slope of the S against T^{-1} plot is almost zero in all cases. This means mechanism (2) of intrinsic conduction is not effective and the $4f^n$ levels lie below the top of the oxygen 2p band. Thus intrinsic band conduction described as mechanism (1) may be the dominant conduction mechanism in these solids. The solid may have electrons or holes as dominant charge carriers depending upon the value of electron and hole mobilities (μ_e and μ_h) and their effective masses ($m_e^*$and m_h^*) in the respective bands. The variation of σ in this model can be given by the relation [15]

$$\sigma = \sigma_0 \exp(-E_g/2kT) \tag{5}$$

where

$$\sigma_0 = 2e(2\pi kT/h^2)^{3/2}(m_e m_h)^{3/4}(\mu_e + \mu_h) = KT^{3/2}a^{3/4}(1 + C)\mu_h m_h^{3/2} \tag{6}$$

with

$$K = 2e(2\pi k/h^2)^{3/2}, \quad a = m_e/m_h \text{ and } C = \mu_e/\mu_h$$

where E_g is the energy band gap and other symbols are the same as explained earlier.

According to this relation, the plot of log σ against T^{-1} in band conduction will be a straight line with a slope of $-E_g/2k$. The variation of log σ with T^{-1} has actually been found to be linear. From these plots values of E_g for cerium, praseodymium, neodymium, samarium, europium and gadolinium vanadates have been obtained and are given in Table IV. On the simple two band model, the variation of S with temperature is given by the relation [16]

$$S = \frac{E_g(C-1)}{2e(C+1)}\frac{1}{T} + 2\left(\frac{C-1}{C+1}\right)\frac{k}{e} + \frac{3}{4}\frac{k}{e}\ln\left(\frac{m_e}{m_h}\right) \tag{7}$$

In band conduction one expects the temperature variation of μ_e and μ_h and m_e and m_h to be similar. It is, therefore, reasonable to assume that their ratios will be constant in the temperature range 400 to T_1'K. Hence the second and third terms in Equation 7, would remain constant with temperature and it can be written as

$$S = \frac{\eta}{eT} + H$$

where

$$\eta = (E_g/2)\left(\frac{C-1}{C+1}\right) \tag{8}$$

and

$$H = 2\left(\frac{C-1}{C+1}\right)\frac{k}{e} + \frac{3}{4}\frac{k}{e}\ln(a) \tag{9}$$

TABLE IV Energy band gap (E_g), the ratio of mobilities (C) and effective masses (a) of electron and holes and their mobilities at 750 K for RVO_4

R	E_g (eV)	c	a	μ_e at 750 K ($m^2V^{-1}sec^{-1}$)	μ_h at 750 K ($m^2V^{-1}sec^{-1}$)
Ce	1.24	0.922	0.144	0.941×10^{-7}	1.023×10^{-7}
Pr	1.28	0.925	1.162	5.887×10^{-9}	6.365×10^{-9}
Nd	1.30	1.080	1.006	1.364×10^{-9}	1.258×10^{-9}
Sm	1.32	1.079	1.330	3.67×10^{-9}	3.38×10^{-9}
Eu	1.34	1.006	1.529	9.12×10^{-9}	3.06×10^{-9}
Gd	1.36	1.109	1.206	4.16×10^{-9}	3.71×10^{-9}

The values of η and H are different for different vanadates and can be obtained from S against T^{-1} plots. The values of E_g are known from electrical conductivity data. Knowing the experimental values of η, H and E_g, both C and a can be evaluated using Equations 8 and 9. From known values of C, and σ_0 one can evaluate the values of μ_h and μ_e in terms of m_h and m_e using Equation 6. The exact values of m_h or m_e are not known for any of these solids; however, one can estimate the values of μ_h and μ_e by taking the mass of the majority charge carrier (hole) to be equal to the mass of a free electron (m_0). Taking $m_h = m_0$, the computed values of μ_h and μ_e together with the values of C and a are also given in Table IV. It is seen from this table that the mobilities of the majority charge carriers (holes) lie in the range 10^{-9} to $10^{-7}\,m^2V^{-1}sec^{-1}$. In normal band conduction one expects the mobility of a charge carrier to be of the order of $10^{-3}\,mV^{-1}sec^{-1}$ or more [17]. Thus evaluated values of mobilities are lower by orders of magnitude. Several reasons, namely the narrow nature of involved bands, neglect of electronic correlation, narrowing of energy bands at higher temperature, scattering of charge carriers by localized magnetic moments, grain boundaries and polaron formation, may lead to lowering of mobility of charge carriers. Out of these, polaron formation seems to be the dominant reason. The polaron concept is well developed [18, 19]. The nature of the involved polaron can be decided by evaluation of a dimensionless coupling constant. Such evaluation favours the formation of a large polaron with intermediate coupling in these solids. The conductivity expression for such a polaron is [19]

$$\sigma = \sigma_0 \exp\left(-\frac{E_g - 2\hbar w_0}{2kT}\right) \quad (10)$$

and for mobility is

$$\mu = \mu_0 \exp(\hbar w_0/kT) \quad (11)$$

where w_0 is the longitudinal optical phonon frequency.

The Seebeck coefficient in the intermediate coupling region also decreases with temperature [20]. Thus the experimental results of σ and S in the light rare-earth vanadates can be explained at least qualitatively using the concept of large polarons with intermediate coupling. The mobility in this case will be much smaller than that of a free electron or hole. It is, however, clear from Equations 1 and 10 that E_a in this case will be equal to $(E_g - 2\hbar w_0)/2$. Here w_0 is expected to be of the order of 10^{13} Hz and gives $2\hbar w_0 \sim 0.13$ eV. Thus the band gap in Table IV should be increased by this amount.

The electrical conductivity of all vanadates except in $GdVO_4$, increases at a much faster rate above T_2. It gives a maximum at T_3 and then sharply drops, shows a minimum around T_4 and then increases with increase in temperature. Table V shows the temperature span (T_3 to T_2), σ at T_2, T_3 and T_4 and its ratio at T_3 and T_2 ($\sigma_{T_3}/\sigma_{T_2}$). For the sake of comparison and discussion, we have included the data on $LaVO_4$ published earlier by us [5]. It is worth mentioning that in $LaVO_4$, electrical conductivity jumps by a factor of 5×10^4 within a temperature span (T_3 to T_2) of 30 K. At T_3 the σ value is of the order of the conductivity of a typical semimetal and is temperature independent above T_3. We have described this as semiconductor–semimetal transition. This transition has been explained as occurring due to lowering of energy band gap between the top of the valence (O^{2-}: 2p) and the bottom of the conduction (V^{5+}: 3d) band and finally their overlap around T_3. Apparently the width of both these bands increases due to

TABLE V Electrical conductivity σ at temperatures T_2 and T_3, their ratios and temperature span (T_3 to T_2) for the RVO_4 studied

R	$\sigma(\Omega^{-1}m^{-1})$ at T_2(K)	$\sigma(\Omega^{-1}m^{-1})$ at T_3(K)	$\sigma_{T_3}/\sigma_{T_2}$	$T_3 - T_2$ (K)	$\sigma(\Omega^{-1}m^{-1})$ at T_4(K)
La	1.53×10^{-4}	7.08	5.0×10^4	30	–
Ce	0.365	4.79	13.2	90	5.25×10^{-2}
Pr	0.027	0.28	10.4	100	3.98×10^{-4}
Nd	0.016	0.16	10.0	90	3.80×10^{-4}
Sm	0.063	0.25	4.0	90	2.29×10^{-4}
Eu	0.151	0.48	3.2	90	9.77×10^{-4}
Gd	0.078	0.22	2.81	80	9.10×10^{-5}

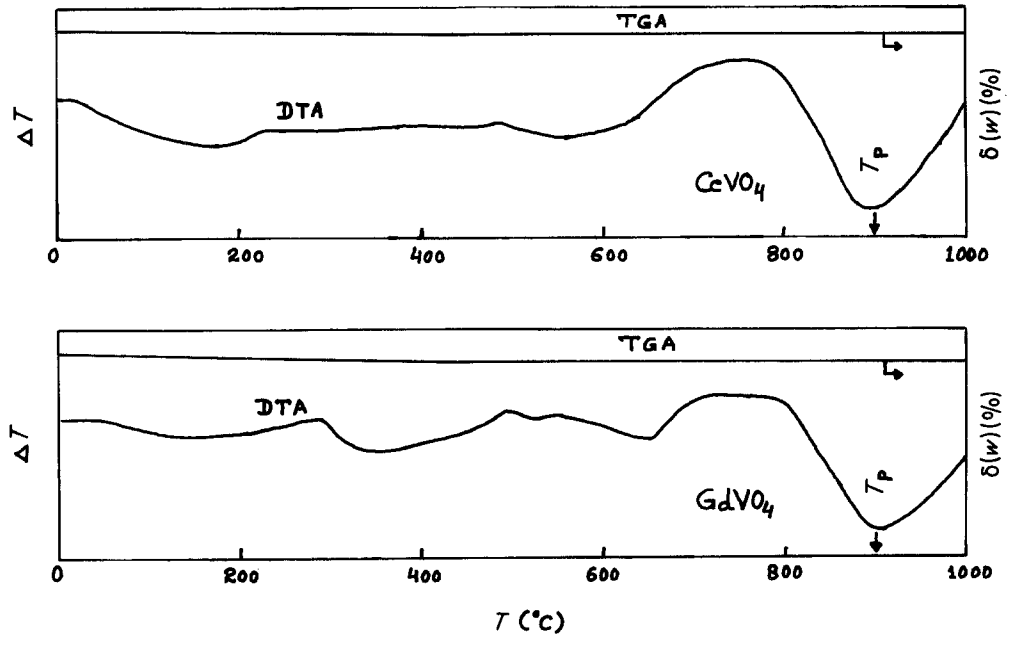

Figure 5 TGA and DTA plots for $CeVO_4$ and $GdVO_4$.

increasing tendency of covalent bonding with increase in temperature. We propose that this tendency of lowering of energy band gap with temperature continues in other members of RVO_4 but the rate of decrease becomes less and less as we go down in the series from lanthanum to gadolinium. This is the reason for the increase of σ above T_2. All rare-earth vanadates tend to become semimetal at higher temperature. However, up to T_3 they could achieve a conductivity which is an order of magnitude less than the value one expects for a semimetal. Both σ at T_3 and the ratio of σ at T_3 and T_2 ($\sigma_{T_3}/\sigma_{T_2}$) decreases (Table V) as we go down in series from lanthanum to gadolinium. The decrease of σ above T_3 and the appearance of minima in the log σ against T^{-1} plot around T_4 (Figs. 1 to 3) for all vanadates seems to be due to phase transition. DTA (shown only for cerium and gadolinium in Fig. 5) shows a peak around 1173 K for different vanadates indicating some sort of structural change in these compounds. We believe that rare-earth vanadates undergo a phase transition around this temperature from low temperature zircon to high temperature scheelite structure. This temperature is not very different from T_4. Thus all vanadates would have become semimetals if their structure was retained up to very high temperatures but this is not the case, and before they could achieve the semimetal state, phase transition throws them back to a less conducting state. It is worth mentioning at this stage that $LaVO_4$, is structurally different from other vanadates. At room temperature it has a monoclinic unit cell (monzite type) against the tetragonal unit cell (zircon type) of other vanadates. The values of energy band gap, T_1 and T_3 to T_2 are thus different for it than others.

Acknowledgements

This work has been supported by CSIR, India. One of us (KG) wishes to thank the Council for financial assistance. The authors are also grateful to Dr D. C. Agrawal, Department of Material Sciences, IIT, Kanpur for DTA and TGA studies, and Dr R. Nagarjan, National Chemical Laboratory, Pune for recording X-ray diffraction patterns.

References

1. G. A. GEHRING and K. A. GEHRING, *Rep. Prog. Phys.* **38** (1975) 1.
2. KANCHAN GAUR, A. K. TRIPATHI and H. B. LAL, *J. Mater. Sci. Lett.* **2** (1983) 161.
3. *Idem, ibid.* **2** (1983) 371.
4. KANCHAN GAUR and H. B. LAL, *ibid.* **2** (1983) 744.
5. *Idem, J. Mater. Sci.* **19** (1984) 3325.
6. R. W. G. WYCKOFF, *Cryst. Struct.* **1** (1965) 17.
7. A. K. TRIPATHI, PhD thesis, Gorakhpur University (1981).

8. A. K. TRIPATHI and H. B. LAL, *J. Mater. Sci.* **17** (1982) 1595.
9. H. B. LAL, B. K. VERMA and V. R. YADAV, *J. Mater. Sci.* **17** (1982) 3317.
10. R. KUMAR, *Sci. Reporter* **8** (1971) 568.
11. A. K. TRIPATHI and H. B. LAL, *Nat. Res. Bull.* **16** (1980) 233.
12. M. F. MOTT, "Metal Insulator Transition" (Taylor and Francis, London, 1974) p. 170.
13. A. K. SAXENA, PhD thesis, Gorakhpur University (1975).
14. J. B. GOODENOUGH, *J. Appl. Phys.* **37** (1966) 1415.
15. C. KITTEL, "Introduction to Solid State Physics", 5th Edn. (Wiley Eastern University, London, 1977) p. 230.
16. T. C. HERMAN and J. M. HONIG, "Thermoelectric and Thermomagnetic Effects and Applications" (McGraw-Hill, New York, 1967) p. 142.
17. J. APPEL, "Solid State Physics", Vol. 21 (Academic Press, New York, 1968) p. 465.
18. I. G. AUSTIN and N. F. MOTT, *Adv. Phys.* **18** (1969) 41.
19. A. J. BOSMAN and H. J. VAN DAAL, *ibid.* **19** (1970) 1.
20. H. SUMI, *J. Phys. Soc. Jpn.* **33** (1972) 327.

Received 26 June
and accepted 15 October 1984